

Optical recording-guided pacing to create functional line of block during ventricular fibrillation

Krishna Ravi
Motoki Nihei
Anjali Willmer
Hideki Hayashi
Shien-Fong Lin

Cedars-Sinai Medical Center
Department of Medicine
Division of Cardiology
and

University of California Los Angeles
David Geffen School of Medicine
Departments of Medicine and Physiology
Los Angeles, California
E-mail: linsf@cshs.org

Abstract. Low-energy defibrillation is very desirable in cardiac rhythm management. We previously reported that ventricular fibrillation (VF) can be synchronized with a novel synchronized pacing technique (SyncP) using low-energy pacing pulses. This study sought to create a line of block during VF using SyncP. SyncP was performed in six isolated rabbit hearts during VF using optical recording to control the delivery of pacing pulses in real time. Four pacing electrodes with interelectrode distances of 5 mm were configured in a line along and across the myocardial fiber direction. The electrodes were controlled independently (independent mode) or fired together (simultaneous mode). Significant wavefront synchronization was observed along the electrode line as indicated by a decrease in variance. With the independent SyncP protocol, the decrease in the variance was 19.3 and 13.7% ($P < 0.001$) for the along-, and across-fiber configurations, respectively. With the simultaneous SyncP protocol, the variance was reduced by 24.2 and 10.7% ($P < 0.001$) in the along- and across-fiber configurations. The effect of synchronization dropped off with distance from the line of pacing. We conclude that SyncP can effectively create a line of functional block that isolates regions of VF propagation. Further optimization of this technique may prove useful for low-energy ventricular defibrillation. © 2006 Society of Photo-Optical Instrumentation Engineers. [DOI: 10.1117/1.2190987]

Keywords: optical mapping; ventricular fibrillation; pacing; defibrillation.

Paper 05155SSR received Jun. 28, 2005; revised manuscript received Oct. 13, 2005; accepted for publication Oct. 13, 2005; published online Apr. 17, 2006.

1 Introduction

The most common method used in the termination of ventricular fibrillation (VF) is the delivery of high-energy shocks. Because these shocks can cause significant pain in patients and require high stored energy, substantial efforts have been devoted to the reduction of defibrillation energy. One approach involves the optimization of shock waveforms and shock timing.¹⁻⁵ A reduction of shock energy by 15 to 50% has been demonstrated through these efforts. Alternatively, a more subtle approach to terminating fibrillation involves the use of electrical pulses to pace the myocardium during the arrhythmia. While this is of great interest and potential benefit, the implementation of such an approach has resulted in varying degrees of success.^{6,7}

During VF, as fibrillatory wavefronts propagate across the surface of a tissue, there are regions of tissue that can still be excited by external stimulation; these regions are known as excitable gaps.^{8,9} The concept of pacing during VF is premised on the use of low-energy pulses to capture the fibrillatory tissue, preferably during the excitable gaps.⁹⁻¹¹ Enlargement of the captured region may eventually lead to VF

termination. The excitable gaps can be captured with a pacing frequency slightly higher than the fibrillation frequency in what is commonly known as "overdrive pacing." However, the limited success of this approach to VF termination may be attributable to the instability of the VF frequency. Pacing with feedback control attempts to deal with the variability of VF frequencies and has shown more promise in tissue capture.^{7,12,13} During feedback pacing, tissue polarization is continuously monitored in real time, thus guaranteeing pacing pulse delivery in the excitable gaps. More importantly, the pacing current is only delivered on activation of a "reference site," which provides a timing reference for wavefront synchronization.

VF propagation can be effectively blocked by creating tissue damage through ablation procedures.^{14,15} These procedures create irreversible tissue damage with unknown long-term consequences. However, functional blocks created without permanently damaging the tissue have not been demonstrated. This study tested the idea of creating a functional block in the ventricle during VF via multiple-electrode configurations. The objective of this study was to apply a synchronized pacing protocol^{7,16} along a linearly distributed array of electrodes to create a linear functional block.

Address all correspondence to Shien-Fong Lin, Cedars-Sinai Medical Center, 8700 Beverly Blvd., Atrium Annex, Rm 108, Los Angeles, CA 90048. Tel: 310-423-7681; Fax: 310-423-0305; E-mail: linsf@cshs.org

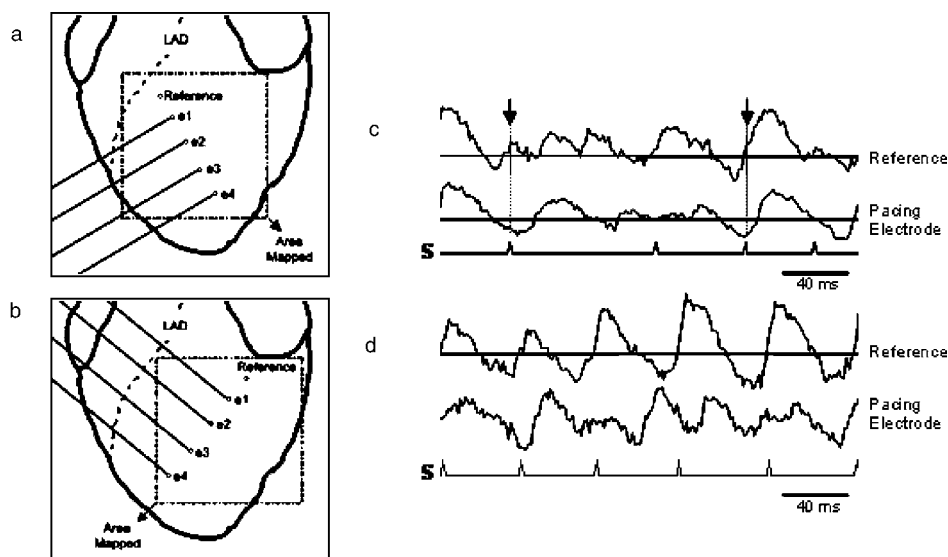


Fig. 1 Pacing protocols. Four unipolar pacing electrodes (e1, e2, e3, and e4) were positioned on the left ventricular anterior wall of the isolated rabbit heart in (a) the fiber direction and (b) cross-fiber direction. A reference site positioned either above e1 or below e4 was used to detect tissue activation. (LAD:left anterior descending coronary artery.) (c) Independent SyncP mode. The first two traces correspond to optical signals registered at a reference site and near a pacing electrode. The third line indicates the time at which an electrical stimulus (S) was delivered through the pacing electrode (d) Simultaneous SyncP mode. All four electrodes fired when activation was detected at the reference site.

2 Materials and Methods

The study protocol was approved by the Institutional Animal Care and Use Committee and followed the guidelines of the American Heart Association.

2.1 Optical Mapping of the Isolated Rabbit Heart

Six New Zealand White rabbits (weight of 3 to 5 kg) were intravenously injected with 1000 units of heparin and anesthetized with ketamine (20 mg/kg) and xylazine (5 mg/kg). After a midline sternotomy, the heart was harvested, and the ascending aorta was cannulated and perfused with 37 °C Tyrode solution (composition in mM: 125 NaCl, 4.5 KCl, 0.25 MgCl₂, 24 NaHCO₃, 1.8 NaH₂PO₄, 1.8 CaCl₂, and 5.5 glucose) gassed with 95% O₂/5% CO₂. Coronary perfusion pressure was regulated between 80 and 95 mmHg, and the hearts were exposed to air. A quadripolar catheter was placed into the endocardium of the right ventricular apex through the pulmonary artery trunk for continuous bipolar recording and the induction of VF. The tissues were stained with 0.5- μ M di-4-ANEPPS (Molecular Probes, Eugene, Oregon). Laser light of 532-nm wavelength (Verdi, Coherent Incorporated, Santa Clara, California) illuminated the tissues, and epifluorescence was collected through a long-pass filter with a cutoff wavelength of 600 nm with a high-speed charge-coupled device camera (430 frames/s, model CA D1-0128T, Dalsa, Waterloo, Ontario, Canada). Image acquisition was controlled by a custom-designed program based on LabView and the IMAQ Vision toolset (National Instruments, Austin, Texas). We mapped the left ventricular anterior wall (20 \times 20 mm²), acquiring 128 \times 128 sites simultaneously. The electromechanical uncoupler cytochalasin D (Sigma Aldrich, Saint Louis, Missouri) was added to the perfusate at a concentration of 5 μ M to inhibit tissue contraction.

2.2 Multielectrode Pacing Protocols

Four pacing electrodes (5 mm apart, Teflon-coated stainless steel with 0.3 mm diam) were placed in the camera's field of view. The electrodes were arranged in a line configuration in along- and across-fiber directions [Figs. 1(a) and 1(b)]. The fiber direction was determined by visual inspection. In the synchronized pacing technique (SyncP) pacing protocol, an additional "reference site" is required in addition to the four physical pacing sites. Two different reference sites were selected at positions in line with the electrodes. The reference site was either above the top electrode (e1) or below the bottom (e4). The reference site was used to determine the timing of activation. The action potentials were monitored optically at sites directly adjacent to (<2 mm) each pacing electrode and the reference site.

Figure 1(c) shows the SyncP algorithm. The main task of the algorithm was to detect the threshold crossing from the optical recordings at the reference site as well as the four pacing sites. Threshold levels were independently set in real time for the reference site and the pacing sites to 40% of the maximum optical potential amplitude. Two types of pacing algorithms were tested. In the independent mode [Fig. 1(c)], each pacing electrode was independently controlled. The pacing current was delivered when the optical potential of the pacing site was below the threshold, and the reference site was depolarized by a VF wavefront to a potential above the threshold level [Fig. 1(c) arrow]. In the simultaneous mode [Fig. 1(d)], all four electrodes fired when activation was detected at the reference site. With this latter mode, we found that at least one of the pacing sites was in the excitable gap in most cases.

VF was induced by endocardial burst pacing in the right ventricle with a pacing cycle length of 50 to 80 ms. The pacing protocol started within one minute of VF induction. We

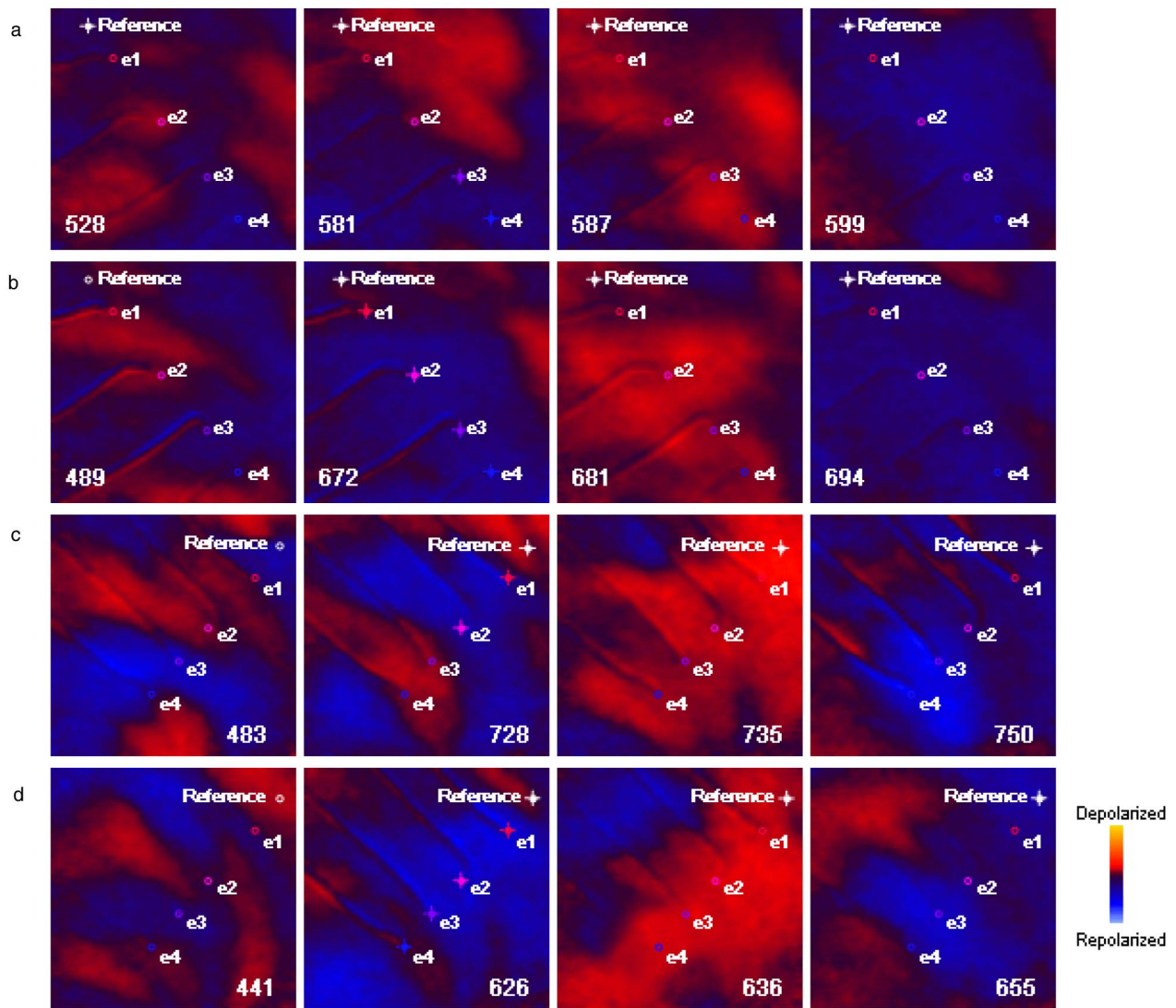


Fig. 2 Voltage maps indicating linear functional block created by SyncP. The red color represents depolarization, and the blue color represents repolarization. Small circles in the maps show locations of the pacing electrodes (e1 through e4). A plus sign in the circle represents the delivery of the pacing current. The frame numbers are indicated in the corners of each map. (a) Independent SyncP, fiber direction; (b) simultaneous SyncP, fiber direction; (c) independent SyncP, cross-fiber direction; and (d) simultaneous SyncP, cross-fiber direction.

recorded 2.3 s (1000 frames: 500 prepacing, 500 pacing) of each pacing protocol by optical mapping. We waited at least 1 min before testing a new electrode configuration or reference site to minimize the effects of the previous pacing protocol. The number of pacing episodes was as follows: independent SyncP, 48 episodes (12 fiber, top reference; 12 fiber, bottom reference; 12 cross-fiber, top reference; 12 cross-fiber, bottom reference); and simultaneous SyncP, 48 episodes (same breakdown as independent SyncP).

2.3 Data Analysis

The variance of optical potential amplitude along the line of pacing electrodes was used to quantify the degree of synchronization. The variance of the action potentials along the electrode line (line interconnecting the reference site and four electrode sites) was calculated for each frame of the prepacing and pacing periods. To calculate the variance, we first normal-

ized the amplitude of the optical signal to values between 0 and 1 for each pixel for each frame. The variance along the electrode line was then obtained from these normalized values. Such an analysis was also performed along lines parallel, but shifted outward from the pacing line to quantify how the effect of pacing drops off with increasing distance from the pacing site.

The VF cycle length was computed at each site along the electrode line as the reciprocal of the frequency peak in the power spectrum on transforming (fast Fourier transform) the action potential to the frequency domain.

3 Results

3.1 Wavefront Synchronization along the Electrode Line

As expected, SyncP caused synchronized activation along the line of pacing electrodes. Figure 2 shows examples of inde-

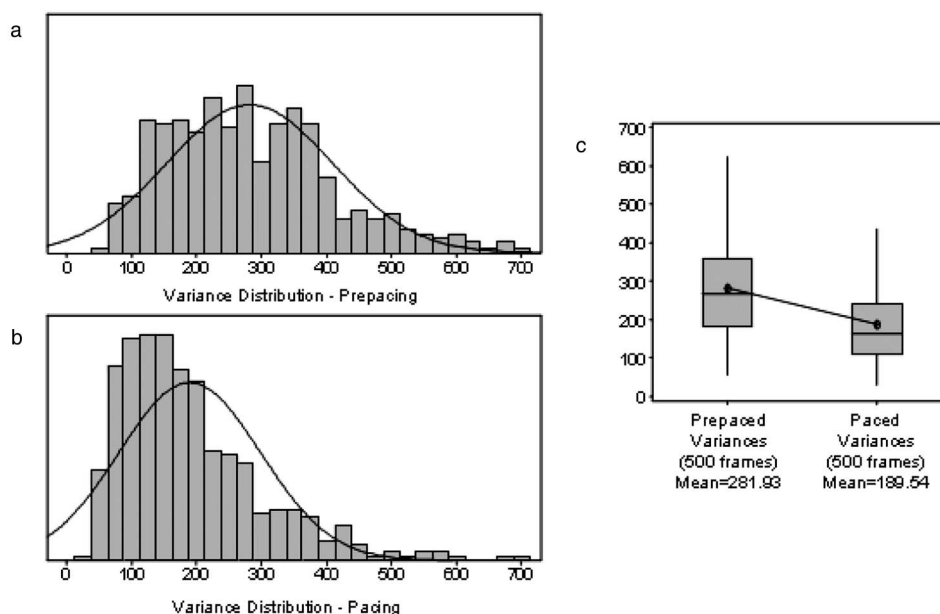


Fig. 3 (a) The variance along the electrode line was calculated for each frame (500 in total) of the pre-pacing period. A graphical summary of the variances is provided by the bell curve (b) Bell curve showing distribution of variances during pacing. The shift of the distribution to the left is indicative of the decrease in variance that occurs with pacing. (c) The box plot quantifies the drop in variance that occurs with the onset of pacing. In this particular trial, the difference in the mean of the variances for the 500 pre-pacing frames and the mean of the variances for the 500 pacing frames is 92.39 with a 95% confidence interval of (77.66, 107.13).

pendent and simultaneous SyncP in the fiber direction [Figs. 2(a) and 2(b)] and cross-fiber direction [Figs. 2(c) and 2(d)]. In Fig. 2(a), when the reference site was activated (frame 581), only sites e3 and e4 were in the excitable gap. Therefore, stimulation current was delivered to e3 and e4, but not to e1 or e2. The stimulation resulted in synchronized activation (frame 587) and repolarization (frame 599). In Fig. 2(b), when the reference site was activated, all electrodes fired at the same time, causing synchronized activation (frame 681) and repolarization (frame 694). The same electrode firing protocols were used in the cross-fiber configuration as shown in Figs. 2(c) and 2(d).

To quantify the change of synchronicity that occurred with pacing, first the variance of the optical signals for every point along the electrode line was calculated for each frame of the pre-pacing period. A graphical summary of the variances during the pre-pacing period is provided by the bell curve in Fig. 3(a) (mean of pre-pacing variances, $\mu_{\text{PREPACING}}=281.93$). The same was done for the pacing period [Fig. 3(b)] ($\mu_{\text{PACING}}=189.54$). The shift of the distribution to the left is indicative of the decrease in variance that occurs with pacing. The drop in variance, representative of increased wavefront synchronization, is visually emphasized by the box plot of Fig. 3(c). The difference in the mean of the variances for the 500 pre-pacing frames and the mean of the variances for the 500 pacing frames ($\Delta\text{variance}=\mu_{\text{PREPACING}}-\mu_{\text{PACING}}=92.39$) was the absolute measure of the effect of pacing on synchronization, and was normalized by dividing by the mean of the variances for the 500 pre-pacing frames to give the percent decrease in variance ($\Delta\text{variance}/\mu_{\text{PREPACING}}=32.8\%$ for Fig. 3).

Figure 4 shows the correlation between wavefront synchronization and variance. The optical traces at sites adjacent

to the electrodes (p1 to p4) are shown in the panels in Figs. 4(a) and 4(d) and reveal an increased synchronicity after the pacing protocol began. The increased synchronicity was not restricted solely to the pacing sites, but also occurred along the line connecting the electrodes. This phenomenon is best illustrated by the space-time plots shown in Figs. 4(b) and 4(e). These plots show the voltage signals at every point along the electrode line (vertical deflection) in time (horizontal deflection). Each horizontal line of varying color is an optical action potential of a single pixel along the electrode line, except the varying voltage amplitudes are instead replaced with varying colors. A homogeneous stripe of color spanning the vertical direction represents the same level of membrane potential depolarization at all points along the electrode line. This observation is quantified by calculating the variance as shown in the panels in Figs. 4(c) and 4(f). The variance of the transmembrane potential for points along the electrode line was calculated for each frame. The synchronization effect is revealed as a relatively smaller variance during pacing compared to the pre-pacing period. In Fig. 4(c), the mean of the variances of the pre-pacing period was 193.12 and the pacing period was 125.54. The decrease in variance by 67.58 ($P < 0.001$) is indicative of the synchronization effect that occurred with pacing. Similarly, in Fig. 4(f), the mean of the pre-pacing variances was 200.80, pacing variances was 143.43, and difference was 57.37 ($P < 0.001$).

3.2 Optimum Electrode Configuration for Pacing

The above-mentioned analysis was extended to all configurations to determine optimum pacing conditions. Figure 5(a) contrasts the amount of synchronization induced by pacing in the fiber and cross-fiber configurations. In both the indepen-

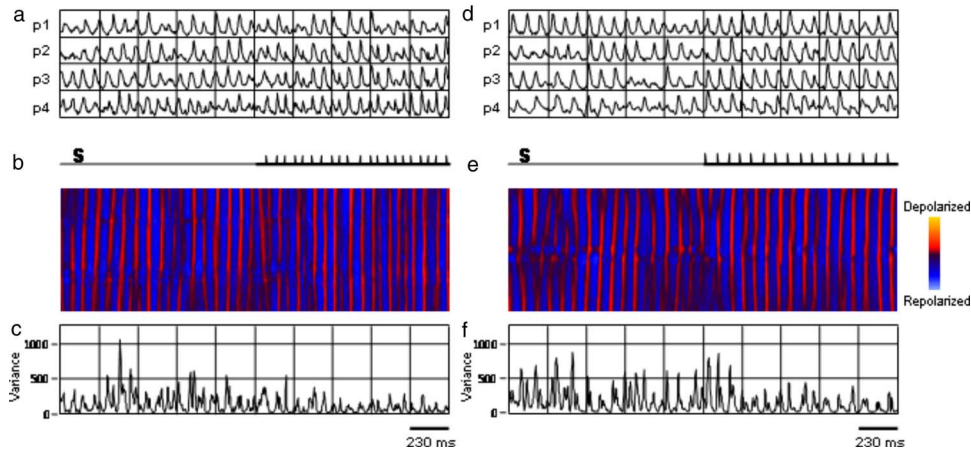


Fig. 4 Effects of SyncP on wavefront synchronization. (a) Optical potentials for four points (p1, p2, p3, p4) situated along an electrode line in the fiber direction. The line marked “S” indicates the time at which an electrical stimulus was delivered through the pacing electrode (simultaneous SyncP). (b) Space-time plot of the optical potential at every point along the electrode line in time. A homogenous stripe of color spanning the vertical direction represents the same depolarization level of optical potential at all points along the electrode line. (c) A plot of the variance in time. Similar action potentials in p1 through p4 tend to correspond to a strip of uniform color in the space-time plot and a small variance. (d), (e), and (f) provide similar plots for a crossfiber, simultaneous SyncP configuration. (c) Variance decrease of 67.58 ($P < 0.001$), from 193.12 prepacing to 125.54 with pacing. (f) Variance decrease of 57.37 ($P < 0.001$), from 200.80 prepacing to 143.43 with pacing.

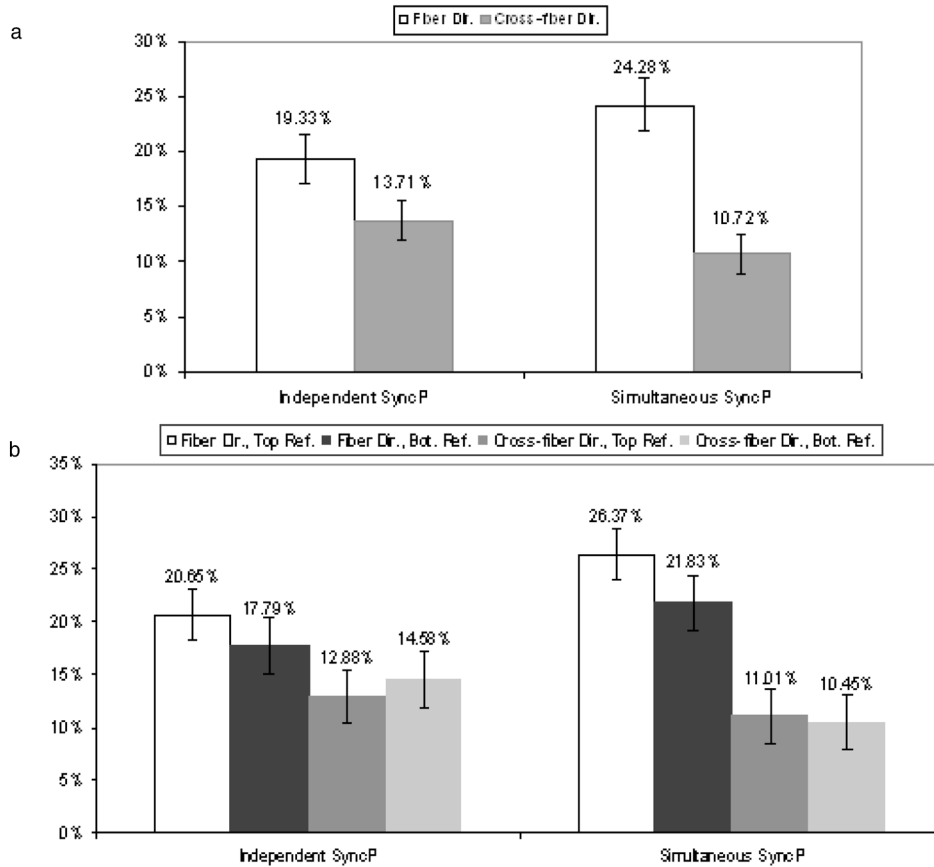


Fig. 5 Decrease in variance due to SyncP pacing with different electrode configurations. Percent decrease in variance = Δ variance/prepacing variance. Δ variance is the difference between the prepacing variance and pacing variance. Large values for percent decrease in variance indicate that pacing has had a strong effect on synchronization. ($P < 0.001$ for all configurations.)

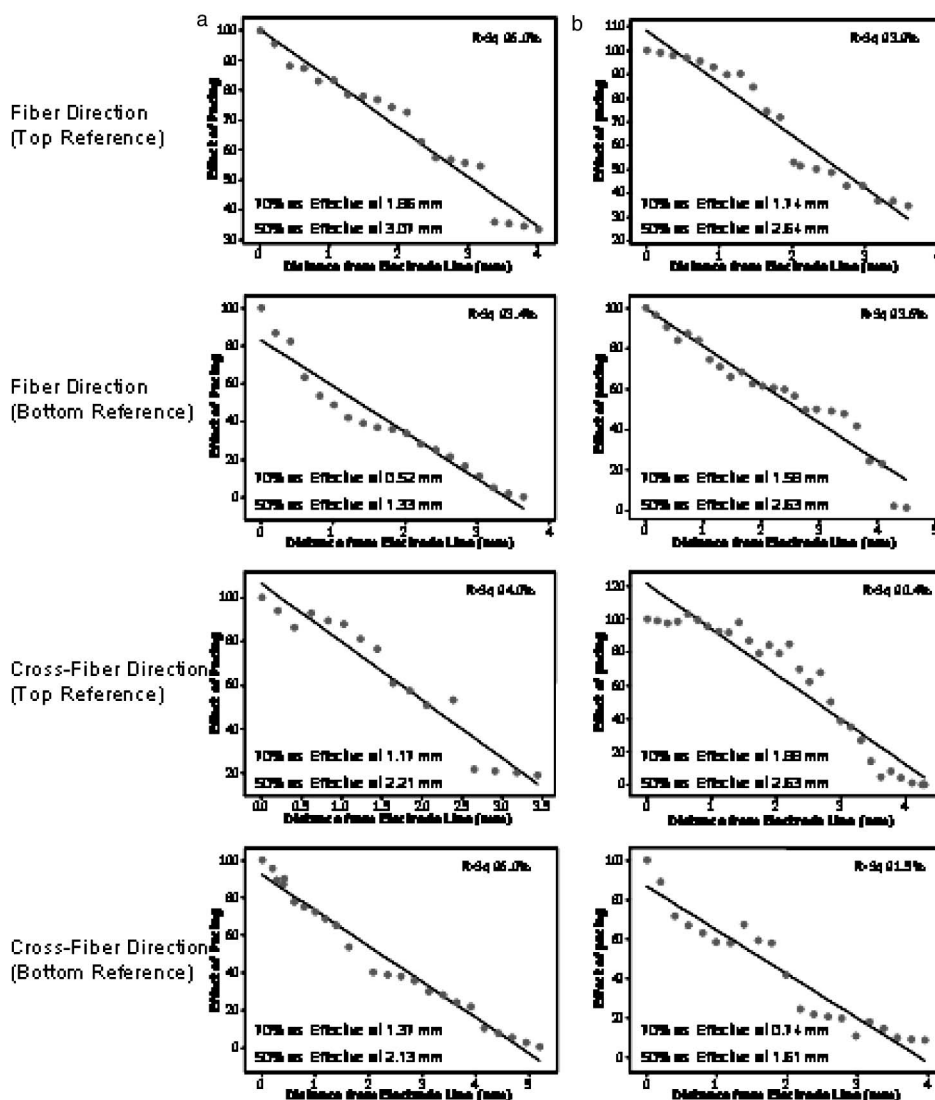


Fig. 6 Effect of pacing drops off with distance from the electrode line. The effect of pacing is measured as the drop in variance between prepacing and pacing periods. A value near 100 indicates a site at which pacing has a strong effect on encouraging wave synchronization, while a value of 0 indicates a site at which pacing has no effect. Values are normalized by dividing variance drops at increasing distances from the electrode line by the variance change (between prepacing and pacing) at the electrode line. (a) Independent SyncP. (b) Simultaneous SyncP. The distances at which the pacing effect drops to 70% and 50% are provided.

dent SyncP and simultaneous SyncP modes, the fiber direction configurations showed a decrease in variance larger than the cross-fiber configurations [independent SyncP: 19.33% decrease in variance (Δ variance=37.89) versus 13.71% (Δ variance=30.72); simultaneous SyncP: 24.28% (Δ variance=47.10) versus 10.72% (Δ variance=24.98), respectively]. (All $P < 0.001$.) In this study, the reference site for the SyncP protocol was placed either above or below the pacing electrodes. The effect of synchronization was compared for these different electrode configurations. Figure 5(b) provides a summary of the synchronization abilities of all eight configurations. Among the configurations in the fiber direction, the simultaneous SyncP protocol proved more effective in the reduction of action potential variance than independent SyncP [top reference: 26.37% decrease in variance (Δ variance=53.26) versus 20.65% (Δ variance=42.33); bot-

tom reference: 21.83% (Δ variance=40.38) versus 17.79% (Δ variance=33.09), respectively]. (All $P < 0.001$.)

3.3 Effect of Pacing Drops Off Linearly with Distance from the Electrode Line

To quantify the variable degree of synchronization (the effect of pacing) away from the electrode line, the drop in variance between prepacing and pacing periods was calculated along lines parallel to, but shifted outward from, the original electrode line. Values were normalized by dividing variance drops at increasing distances from the electrode line by the variance change (between prepacing and pacing) at the electrode line. A value near 100 indicates a site at which pacing has a strong effect on encouraging wave synchronization, while a value of 0 indicates a site at which pacing has no effect.

Figures 6(a) and 6(b) show the linear dropoff in synchronization that occurred with pacing along an electrode line for the independent and simultaneous SyncP, respectively. In the independent SyncP mode, pacing was 70% as effective at 1.2 mm and 50% as effective at 2.2 mm. In the simultaneous SyncP mode, the amount of synchronization dropped to 70% at 1.5 mm, and to 50% at 2.4 mm.

4 Discussion

In this study, we demonstrate a novel means for the creation of linear functional block during VF by the application of the SyncP protocol in both along- and across-fiber directions. Pacing in the fiber direction with the reference site on top of the electrodes appeared to be most effective in causing wavefront synchronization along the pacing line. The pacing effect of enhanced synchronicity dropped off in a linear fashion when the synchronicity was measured at increasing distances from the pacing line. Previous applications^{7,16} of the SyncP pacing protocols created an area of synchronized propagation, whereas the current technique created a synchronized line. A major difference between these two approaches is that while area synchronization of VF wavefronts resulted in a 16% termination rate,⁷ we did not observe termination of VF with the linear electrode configurations.

We previously implemented a synchronized pacing protocol to explore the possibility of synchronizing VF propagation using low-energy pacing pulses. The SyncP approach has been shown experimentally to be eight times more likely to terminate ventricular fibrillation than simple overdrive pacing.⁷ Wavefront synchronization and synchronization of repolarization are important for VF termination. Experimental and theoretical studies^{7,17} showed that pacing during the excitable gaps helps decrease the dispersion of VF activations, extinguishing the vortex by moving it to an inexcitable boundary, leading to VF termination. At least two mechanisms have been proposed to explain the defibrillation effect of synchronized pacing. One possible explanation of the defibrillation mechanism of SyncP proposed by the Pak et al. study was the electrical reduction of available tissue mass to sustain VF. Although SyncP did not mechanically reduce tissue mass, pacing could have induced a virtual reduction of tissue mass that enlarged the synchronized area and decreased the dynamic complexity of VF, leading to the termination of fibrillation. Another possibility is that pacing in the dominant tissue area that is likely to exhibit a “mother rotor” behavior that can suppress VF conduction.

The objective of the current study was to create a functional line of block with the SyncP approach, not aiming directly at VF termination. Our results showed that the synchronization effect dropped off rapidly away from the pacing line. Consequently, a virtual reduction of tissue mass was not achieved with the linear electrode configuration. Furthermore, a line configuration of pacing electrodes cannot cover a dominant area of VF. The combined effects might explain the lack of VF termination in the current study. An important finding of this study is that the frequency content of VF at the reference site appears to play an important role in determining the efficacy of functional block creation. The averaged dominant frequency of the reference site before pacing was 18.1 Hz near the base LV and 17.5 Hz near the apex. The faster VF in

the basal LV might explain the higher efficacy of functional block creation when the reference site was placed at the top of the pacing electrodes.

The recent advancement of catheter design and pacing technology has allowed pacing with multiple, spatially distributed electrodes. Byrd et al.¹⁸ showed that biventricular anti-tachycardia pacing is superior to conventional antitachycardia pacing in situations where the additional ventricular lead advanced the orthodromic wavefront. This advancement may increase the likelihood of orthodromic termination at refractory tissue and termination of reentry. As many ICDs have an additional lead available for pacing, this concept of biventricular pacing might also prove beneficial for VF termination via increased capture area and increased conduction blocks. While in our study, pacing only occurred in the left ventricle, it is possible for our SyncP protocol to elicit the necessary orthodromic wavefront necessary for reentry termination.

Linear electrode arrays are preferable in clinical situations, because they can be placed on a catheter. Newton et al.⁶ found that by using a pulse train of fixed frequencies, electrodes in a linear configuration were more capable of capturing the tissue than point electrodes during VF. A recent study demonstrated that pacing in the posterior LV resulted in a greater incidence and extent of LV capture than stimulation from the anterior LV.¹⁹ SyncP was applied only to the anterior LV in this study. If the directionality of fibrillatory propagation also exists in the rabbit ventricles, as in the case of swine, then pacing in the posterior LV may be a better strategy for the application of SyncP in defibrillation. Furthermore, we created only one line of functional block in this study. It is feasible to create multiple lines of functional block with this approach. Note that the successful defibrillation rate with our previous area synchronization approach was only 16%.⁷ This rate may be significantly increased through a combination of area and linear synchronized pacing methods.

Acknowledgments

This study was supported by the American Heart Association (including a summer student fellowship to Ravi, a postdoctoral fellowship to Nehei, and a Scientist Development Award to Hayashi) NIH/NHLBI HL58533, SCOR in Sudden Cardiac Death P50 HL52319.

References

1. S. R. Shorofsky, A. H. Foster, and M. R. Gold, “Effect of waveform tilt on defibrillation thresholds in humans,” *J. Cardiovasc. Electrophysiol.* **8**, 496–501 (1997).
2. J. Jones, W. Noe, O. Tovar, Y. Lin, and W. Hsu, “Can shocks timed to action potentials in low-gradient regions improve both internal and out-of-hospital defibrillation?” *J. Electrocardiol.* **31**, 41–44 (1998).
3. R. A. Malkin, “Large sample test of defibrillation waveform sensitivity,” *J. Cardiovasc. Electrophysiol.* **13**, 361–370 (2002).
4. R. G. Walker, B. H. Kenknight, and R. E. Ideker, “Critically timed auxiliary shock to weak field area lowers defibrillation threshold,” *J. Cardiovasc. Electrophysiol.* **12**, 556–562 (2001).
5. C. Butter, E. Meisel, J. Tebbenjohanns, L. Engelmann, E. Fleck, B. Schubert, S. Hahn, and D. Pfeiffer, “Transvenous biventricular defibrillation halves energy requirements in patients,” *Circulation* **104**, 2533–2538 (2001).
6. J. C. Newton, J. Huang, J. M. Rogers, D. L. Rollins, G. P. Walcott, W. S. Smith, and R. E. Ideker, “Pacing during ventricular fibrillation: factors influencing the ability to capture,” *J. Cardiovasc. Electrophysiol.* **12**, 76–84 (2001).
7. H. N. Pak, Y. B. Liu, H. Hayashi, Y. Okuyama, P. S. Chen, and S. F.

- Lin, "Synchronization of ventricular fibrillation with real-time feedback pacing: implication to low-energy defibrillation," *Am. J. Physiol. Heart Circ. Physiol.* **285**, H2704–H2711 (2003).
8. B. H. KenKnight, P. V. Bayly, R. J. Gerstle, D. L. Rollins, P. D. Wolf, W. M. Smith, and R. E. Ideker, "Regional capture of fibrillating ventricular myocardium: Evidence of an excitable gap," *Circ. Res.* **77**, 849–855 (1995).
 9. T. Taneja, G. Horvath, D. K. Racker, J. Goldberger, and A. Kadish, "Excitable gap in canine fibrillating ventricular myocardium: effect of subacute and chronic myocardial infarction," *J. Cardiovasc. Electrophysiol.* **12**, 708–715 (2001).
 10. K. Kamjoo, T. Uchida, T. Ikeda, M. C. Fishbein, A. Garfinkel, J. N. Weiss, H. S. Karagueuzian, and P. S. Chen, "Importance of location and timing of electrical stimuli in terminating sustained functional reentry in isolated swine ventricular tissues: evidence in support of a small reentrant circuit," *Circulation* **96**, 2048–2060 (1997).
 11. Y. Gu and A. Patwardhan, "Multiple spatially distributed stimulators and timing programs for entrainment of activation during ventricular fibrillation," *Biomed. Sci. Instrum.* **38**, 295–299 (2002).
 12. R. Wu and A. Patwardhan, "Restitution of action potential duration during sequential changes in diastolic intervals shows multimodal behavior," *Circ. Res.* **94**, 634–641 (2004).
 13. P. N. Jordan and D. J. Christini, "Adaptive diastolic interval control of cardiac action potential duration alternans," *J. Cardiovasc. Electrophysiol.* **15**, 1177–1185 (2004).
 14. D. Keane, "New catheter ablation techniques for the treatment of cardiac arrhythmias," *Card. Electrophysiol. Rev.* **6**, 341–348 (2002).
 15. H. N. Pak, Y. S. Oh, Y. B. Liu, T. J. Wu, H. S. Karagueuzian, S. F. Lin, and P. S. Chen, "Catheter ablation of ventricular fibrillation in rabbit ventricles treated with beta-blockers," *Circulation* **108**, 3149–3156 (2003).
 16. H. N. Pak, Y. Okuyama, Y. S. Oh, H. Hayashi, Y. B. Liu, P. S. Chen, and S. F. Lin, "Improvement of defibrillation efficacy with preshock synchronized pacing," *J. Cardiovasc. Electrophysiol.* **15**, 581–587 (2004).
 17. T. Ashihara, T. Namba, M. Ito, T. Ikeda, K. Nakazawa, and N. Trayanova, "Spiral wave control by a localized stimulus: a bidomain model study," *J. Cardiovasc. Electrophysiol.* **15**, 226–233 (2004).
 18. I. A. Byrd, J. M. Rogers, W. M. Smith, and A. E. Pollard, "Comparison of conventional and biventricular antitachycardia pacing in a geometrically realistic model of the rabbit ventricle," *J. Cardiovasc. Electrophysiol.* **15**, 1066–1077 (2004).
 19. K. Nanthakumar, P. L. Johnson, J. Huang, C. R. Killingsworth, D. L. Rollins, H. T. McElderry, W. M. Smith, and R. E. Ideker, "Regional variation in capture of fibrillating Swine left ventricle during electrical stimulation," *J. Cardiovasc. Electrophysiol.* **16**, 425–432 (2005).